PREDICTION OF PRESSURE DROP IN FLUID TUNED MOUNTS USING ANALYTICAL AND COMPUTATIONAL TECHNIQUES

William C. Lasher*, Amir Khalilollahi*, John Mischler**, Tom Uhric**
The School of Engineering and Engineering Technology
The Pennsylvania State University at Erie, The Behrend College
Station Road, Erie, Pa. 16563

ABSTRACT

A simplified model for predicting pressure drop in fluid tuned isolator mounts has been developed. The model is based on an exact solution to the Navier-Stokes equations and has been made more general through the use of empirical coefficients. The values of these coefficients were determined by numerical simulation of the flow using the commercial CFD package FIDAP.

INTRODUCTION

Fluid-tuned mounts [1] are an effective device for vibration isolation. A simple mount consists of fluid filled chambers connected by a narrow inertia track (Figure 1). When a force is applied to the chamber ends, the fluid is forced through the inertia track causing a pressure drop across the mount. The magnitude and phase of the pressure drop are important parameters in determining the isolation performance of the mount. It is possible to tune the mounts to a specific "notch frequency" by varying the geometric shape of the mount. The shape of the mount and the flow parameters determine the flow resistance, which determines the notch frequency. The design problem then becomes one of determining the shape and flow parameters for a specific notch frequency. This is a complicated fluid dynamics problem; successful design of the mounts requires either sophisticated computational fluid dynamics (CFD) predictions or construction of prototypes for experimental testing. Either of these options requires a considerable amount of time and resources, which makes them difficult to use as design tools. Although this analysis and testing cannot be completely avoided, a simplified empirical model would allow the designer to investigate the effects due to changes in important parameters, and perform preliminary screening on different proposals.

In the present work a model is developed for the simplified geometry shown in Figure 2. The problem can be non-dimensionalized using the mean velocity u_0 and diameter d of the inertia track. The non-dimensional parameters are defined as:

---

* Assistant Professor of Mechanical Engineering

** Undergraduate Student Research Assistant

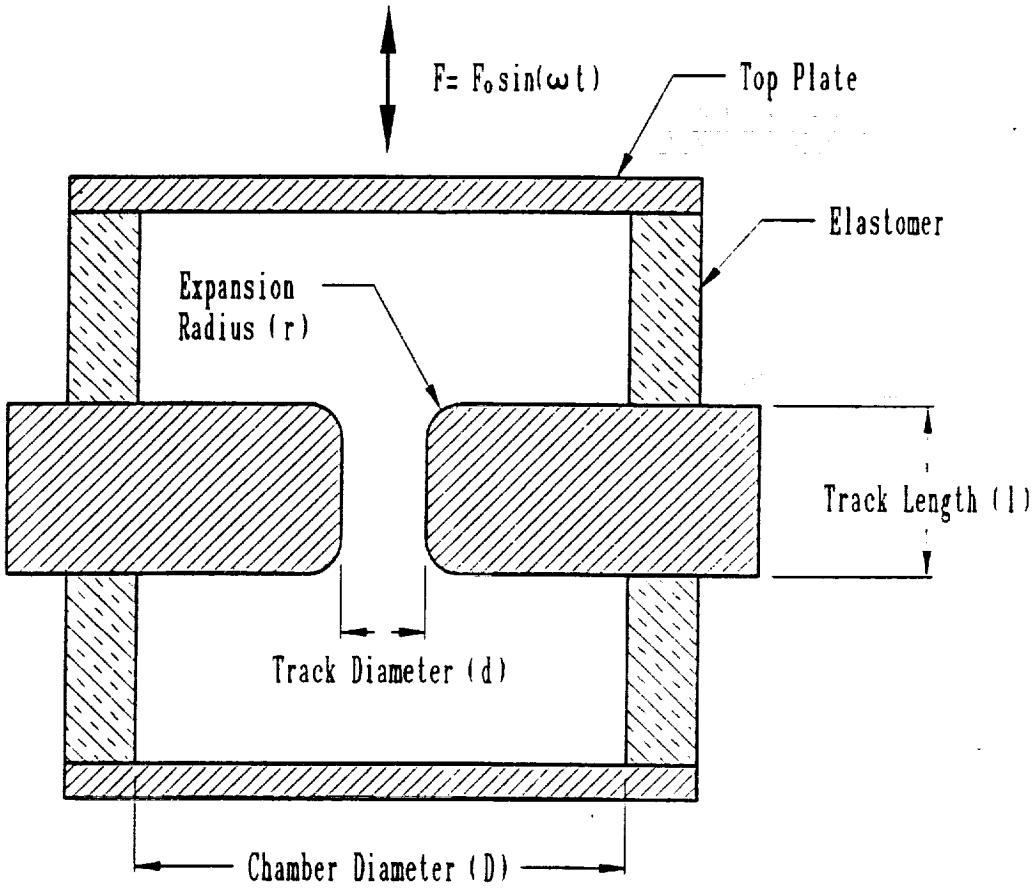

Figure 1
Simple Mount

D/d: expansion ratio
l/d: length/diameter ratio
r/d: radius/diameter ratio
Re: Reynolds Number ($\rho u_o d/\mu$)
St: Strouhal Number ($\omega d/u_o$)
Va: Valenci Number (Re•St)

where

ρ = density
μ = viscosity
ω = angular frequency

A theoretical model for predicting the pressure drop for this geometry was previously developed. The model consists of a series of component models (inertia track, expansion, contraction, and end chamber) which contain coefficients that must be determined by experiment or numerical simulation. In the present work a series of numerical simulations were performed to determine the value of these coefficients, which are a function of mount

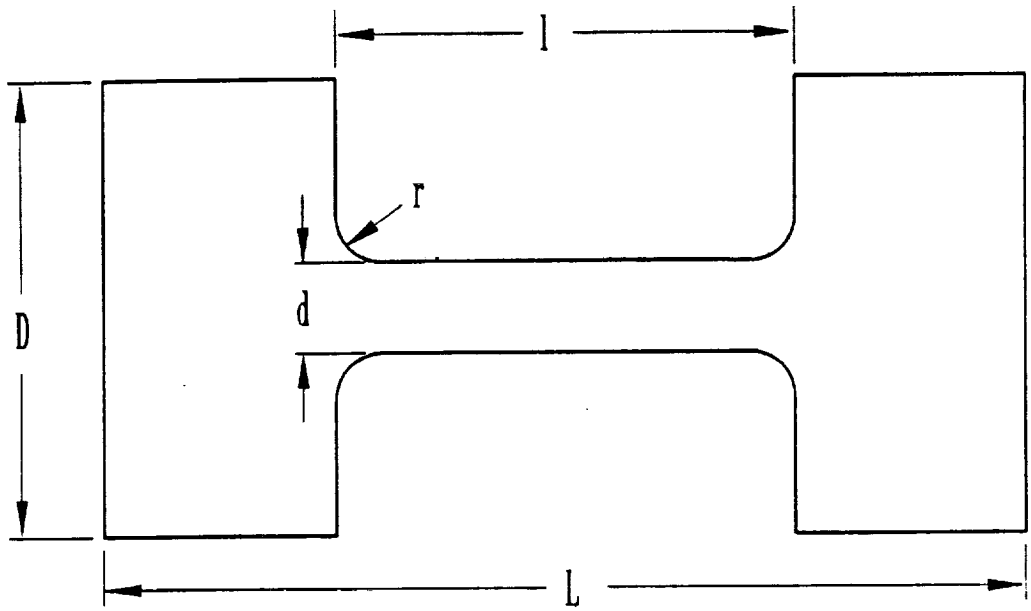

Figure 2
Simplified Mount Geometry

geometry and flow parameters. Completion of the model will require experimental verification, which is in progress.

MATHEMATICAL MODEL

A control volume analysis on the simplified geometry of Figure 2 gives the following equation:

$$A_0 \Delta P = \rho l \frac{dQ}{dt} + F_b \tag{1}$$

where A_0 is the cross-sectional area of the end chambers, P is the pressure, Q is the volume flow rate, and F_b includes the effects of viscous shear, expansion/contraction, and other forces such as body and gravity forces. This equation simply states that the resistance to the pressure difference across the mount is determined by the inertia of the fluid and a general shear/body force.

Presently, the force F_b includes two effects: the viscous resistance, and expansion/contraction terms. The latter are minor contributors and are [2]:

$$\Delta P_{con} / \left(\frac{1}{2}\rho u_0^2\right) = 0.42\left(\frac{1}{A} - \frac{1}{A_0}\right) \tag{2}$$

$$\Delta P_{exp} / \left(\frac{1}{2}\rho u_0^2\right) = \left(1 - \frac{A}{A_0}\right)^2 \tag{3}$$

where A is the cross-sectional area of the inertia track.

The major part of the resistance to the flow occurs within the relatively long inertia track and the end chambers, where the spatial and periodic velocity components exist. The analysis of the oscillatory viscous flow through uniform pipes can be favorably applied to develop the relation between the flow rate and pressure difference across the mount. This phasor relation includes the effects of viscous shear as well as the inertia of the fluid. If a long circular cross-section pipe of radius R undergoes an oscillatory pressure gradient, the volume flow rate through this pipe is [3]:

$$Q = \frac{\pi R^2 \Delta P_0}{\rho l i \omega}\left(1 - \frac{2\alpha i^{3/2} J_1(\alpha i^{3/2})}{i^3 \alpha^2 J_0(\alpha i^{3/2})}\right) e^{i\omega t} \tag{4}$$

where α is equal to $R(\omega/\nu)^{1/2}$ and is referred to as the frequency parameter (α^2 is equivalent to Va/4). J_0 and J_1 are Kelvin functions [4].

It is practical to input the displacement of the mount rather than the force on the mount. In this case the volume flow rate is known

$$Q = Q_0 \sin(\omega t) \tag{5}$$

and the pressure difference ΔP must be calculated from:

$$\Delta P = R_F Q_o \sin(\omega t + \phi) \tag{6}$$

Using the above analytical solution and after some arrangement [5], the unknowns R_F and ϕ are obtained:

$$|Z| = R_F = \frac{\rho \omega l}{\pi R^2 M_{10}} \tag{7}$$

$$\phi = \frac{\pi}{2} - \epsilon_{10} \tag{8}$$

where R_f is the magnitude of the impedance to the flow, and

$$M_{10} = \frac{1}{k}\sqrt{\sin^2\delta_{10} + (k - \cos\delta_{10})^2} \tag{9}$$

$$\delta_{10} = \frac{3\pi}{4} - \theta_1 + \theta_o \tag{10}$$

$$\epsilon_{10} = \tan^{-1}\left(\frac{\sin\delta_{10}}{k - \cos\delta_{10}}\right) \tag{11}$$

$$k = \frac{\alpha M_0}{2M_1} \tag{12}$$

The final assembly of components used in the characterization of the mount impedance is represented by a series circuit diagram (Figure 3) where Q (as current) creates ΔP (as a potential). The theoretical flow impedance of the inertia track, Z, and that of the chambers, Z_0, includes both the inertial and viscous forces that can be found by equations (7) and (8), and are complex values. The contraction/expansion terms are assumed to have negligible inertial resistance but they add to the viscous resistance, so their impedances have only real components. They can be approximated as

$$Z_{con} = \frac{\rho Q_o^2}{2}\left(\frac{1}{A} - \frac{1}{A_o}\right) \tag{13}$$

$$Z_{exp} = \frac{\rho Q_o^2}{2}\left(1 - \frac{A}{A_o}\right)^2 \tag{14}$$

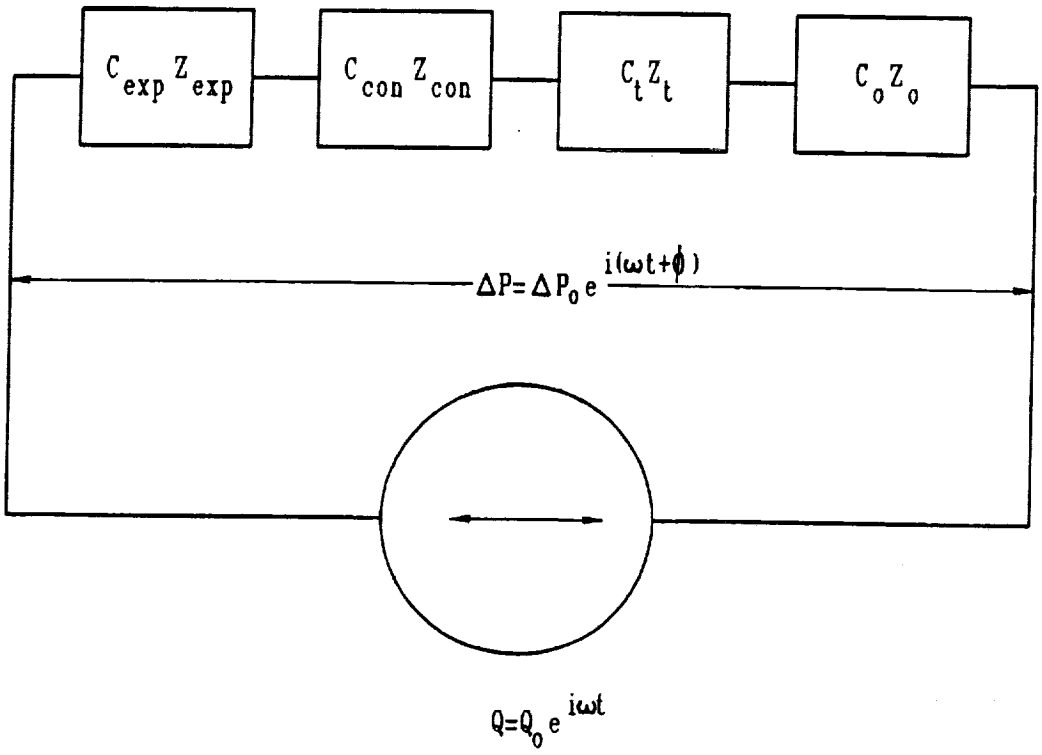

Figure 3
Schematic Representation of Flow Impedances

The total instantaneous pressure difference can be stated as the sum of contributing phasors:

$$\Delta P = (C_{exp}Z_{exp} + C_{con}Z_{con} + C_cZ_c + C_tZ_t)Q \qquad (15)$$

The empirical coefficients (C's) are discussed and algebraicly evaluated later in terms of different flow geometries and frequency parameters, upon comparison with the results from numerical simulations.

NUMERICAL COMPUTATIONS

The reason for performing numerical simulations is to extend the range of applicability of the previously described model. For example, the model for the inertia track was developed for infinite length pipes. Simulation of flow in a pipe of finite length provides a correction factor which may be used in predicting the pressure drop for a realistic geometry.

Two computational domains were studied in the present work. In order to determine

coefficients for finite track length and expansion/contraction losses, it is necessary to simulate the full mount, as shown in Figure 4. The problem is axi-symmetric, with the axis of symmetry along the centerline of the inertia track. The boundary conditions are set to zero velocity, except at the ends, where a periodic normal velocity is specified. A systematic series of computations was performed, varying the ratio of track length to diameter and contraction/expansion corner radii.

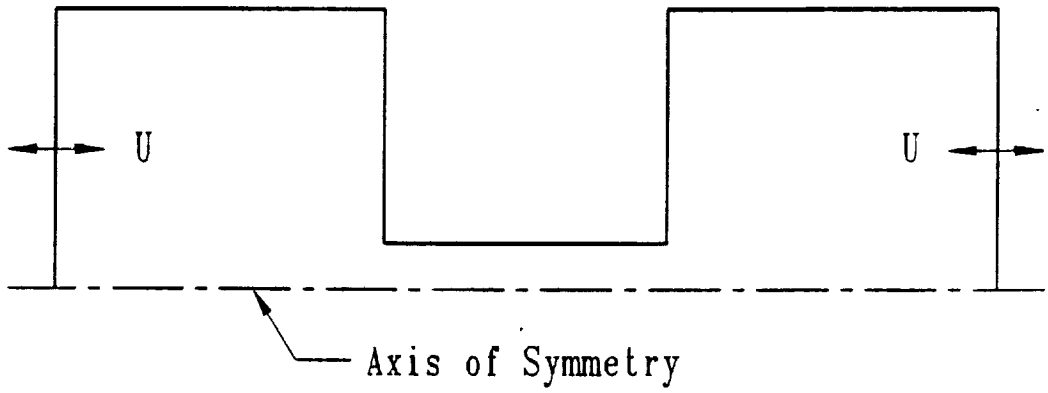

Figure 4
Computational Domain for Full Mount

To determine the effect of different cross-sectional inertia track shapes on pressure drop, the domain shown in Figure 5 was studied. This corresponds to the infinite length pipe by setting the end conditions to zero normal velocity gradient and applying a periodic pressure difference. There are two advantages of this approach over specifying periodic normal velocity - only one element is needed in the x-direction, since all x-derivatives are zero; and the problem is linear, since the convective terms are zero. These advantages greatly reduce the computational time required for solution, which is important when the simulations are for non-circular cross-section, because they must be fully three-dimensional. The disadvantage of this approach is that the flow parameters (i.e., Reynolds number and Strouhal number) are not known until the problem has been solved. In the present work the theoretical model is used to find an approximate pressure drop for non-circular cross sections corresponding to the desired flow parameters. This pressure drop is then used as input, and the exact flow parameters are determined from the simulation.

The incompressible Navier-Stokes equations are solved using the Galerkin formulation of the Finite Element Method provided in the CFD package FIDAP [6]. Each problem was started with an initial velocity of zero. For the full mount case, each problem was run until the pressure history became periodic, which generally occurred in 3 cycles or less. For the infinite length track case, each problem was run until the volumetric flow rate became periodic, which generally occurred in 20 cycles or less.

For each case a preliminary numerical study was performed to optimize FIDAP options. Grid independence was determined for a typical case by doubling the number of elements until there was less than 2% difference in the predicted pressure drop or flow rate.

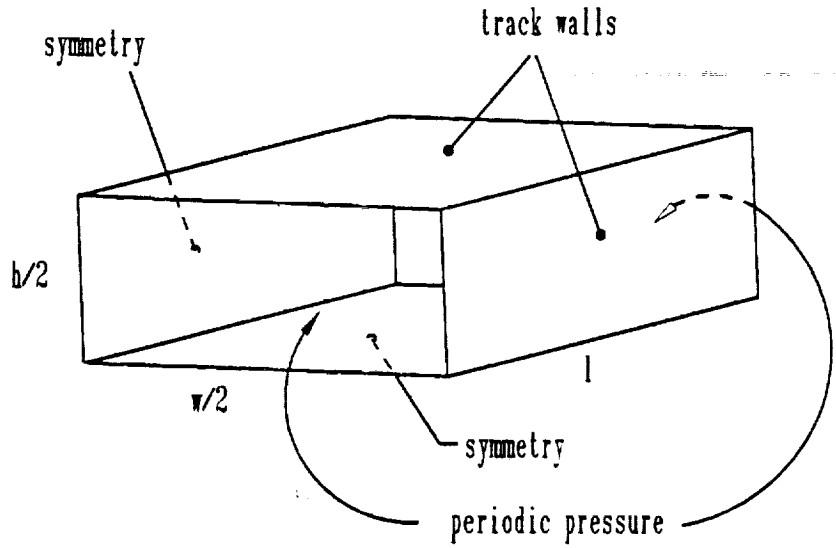

Figure 5
Computational Domain, 3-D Rectangle

The optimal time increment was determined in a similar manner to be 50 time steps per cycle. An acceleration factor of 0.5 was used along with the quasi-Newton solver. The penalty formulation was used for pressure, with the penalty parameter set to 10^{-9}. For the higher Reynolds number cases (above 100) the upwinding option was used to suppress oscillations in the computed velocity field. Backward integration was used for the time derivative.

All of the simulations reported here are for laminar flow. Turbulent simulations for a few cases were performed, but the results were later abandoned for two reasons. First, it is unclear whether the conditions typically found in fluid tuned mounts are in fact turbulent. Ahn and Ibrahim [7] discuss the results of several studies that show transition Reynolds number for periodic flow increases with increasing frequency. The high frequencies typically found in mounts cause the fluid to move as a slug with extremely thin shear layers at the walls. For the frequencies and Reynolds numbers of interest in the present work, the formulas presented by Ahn and Ibrahim indicate laminar flow. Experimental work is in progress to determine if this is in fact the case.

The second problem is that simulation of unsteady turbulent flow is problematic because the k-e turbulence model is based on steady flow, and may not be applicable to oscillating flows. Lasher and Taulbee [8] discuss this problem in more detail. In addition, the form of the model used in FIDAP is a high-Reynolds number model that uses wall functions, and therefore cannot predict transition. As a result of these concerns, turbulent simulations have been deferred until experimental data is available.

FIDAP generally works quite well on this problem, although there were a few difficulties. One of the most significant problems is that the pressure history sometimes developed unrealistic oscillations when the second-order trapezoidal integration was used for the time derivative, which caused the solution to diverge. As a result, the simulations were

performed using the less-accurate backward integration. This is a known problem with the penalty formulation for the pressure, but was unexpectedly found to also occur when the segregated solver (which solves the Poisson equation for the pressure) was used. This problem is currently under investigation.

Simulations were also attempted using FLUENT [9]; however, these did not work as well as FIDAP. It took significantly longer to get a converged solution, and it was found that the interpolation done by the program for time-varying boundary conditions is incorrect. The results obtained by FLUENT did agree well with those obtained by FIDAP.

DETERMINATION OF EMPIRICAL COEFFICIENTS

The empirical coefficients of Equation 15 are developed in terms of nondimensional geometric and flow parameters. Using the pressure drop predicted across a component by computational simulation, the coefficient is found as

$$C = \frac{\Delta P_{computational}}{\Delta P_{model}} \tag{16}$$

Certain geometric components contribute to the flow resistance more than others. Figure 6 shows the centerline pressure drop across a typical mount.

Because most of the pressure drop across the mount occurs in the inertia track, the track component will be the most significant. The pressure drop across the expansion and contraction typically represents 6-10% of the total pressure drop shown. The pressure drop across the chamber is relatively small, so any difference between the model and computational results will not be significant in the overall pressure drop. The chamber coefficient is therefore set to 1. In general the coefficients will be functions of several parameters, such as Reynolds number, Strouhal number, etc. We assume that the coefficients are separable into individual coefficients for each parameter; for example:

$$C = C(R_e) \cdot C(S_t) \cdot C(l/d) \tag{17}$$

RESULTS

Expansion/Contraction Coefficients

Within each cycle, the expansion becomes the contraction and vise versa. Because of this, the expansion and contraction losses are combined as a single loss. The coefficient will be dependent on the following nondimensional geometric and fluid parameters:

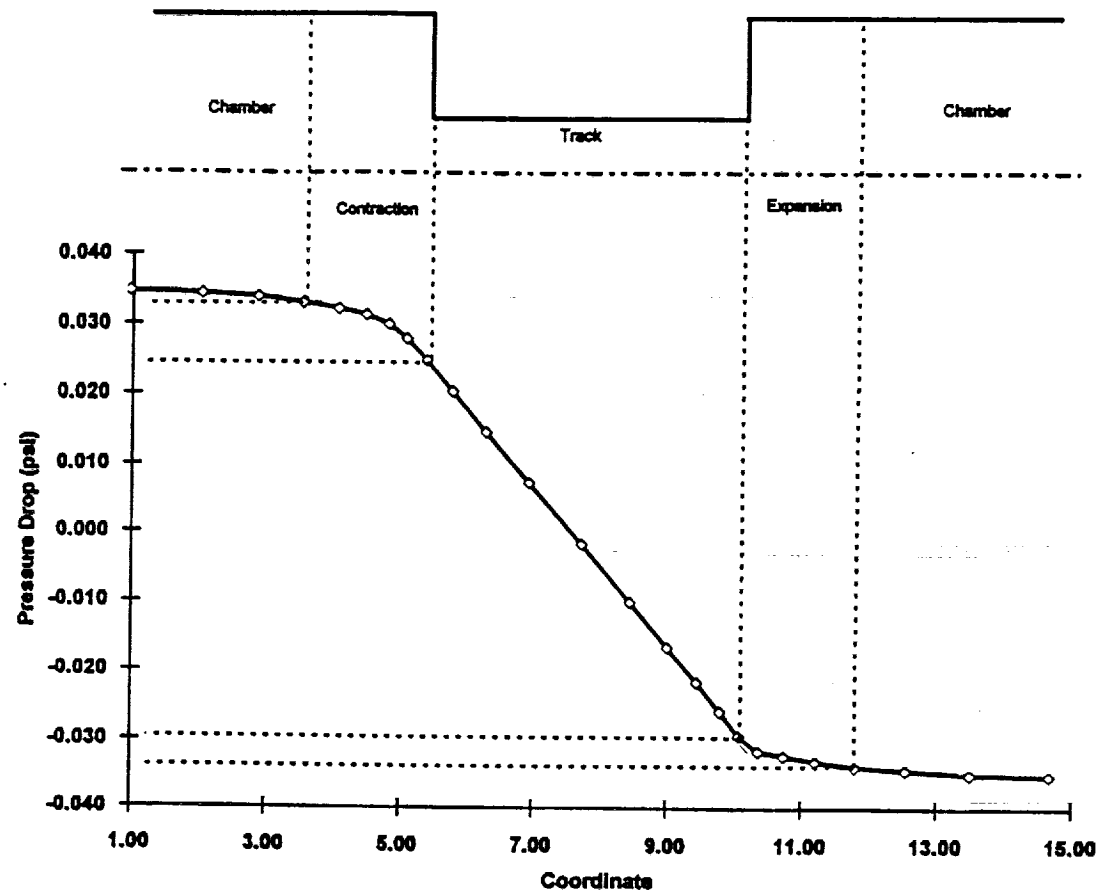

Figure 6
Typical Centerline Pressure Drop

D/d = Expansion Ratio
Re = Reynolds Number
St = Strouhal Number
r/d = Expansion Radius to Diameter Ratio

First, the Reynolds number dependence is considered. In the development of the theoretical model, the pressure drop across the expansion is formulated from the x-momentum equation. The momentum equation contains a viscous term for the wall shear stress, which is neglected in the derivation. If the viscous term is carried through the derivation, it becomes equivalent to adding a term to the nondimensional pressure drop which is proportional to the inverse of the Reynolds Number. Simulations were performed at an expansion ratio of 5 for Reynolds numbers of 1, 10, 100 and 1000. The coefficient was determined by taking the difference between the model and computation and performing a least-squares regression. The resulting corrective term is:

$$A(R_e) = \frac{0.0825}{R_e} \tag{18}$$

The data points and equation (18) are shown in Figure 7. Note that the term asymptotically approaches zero as the Reynolds number increases, as expected.

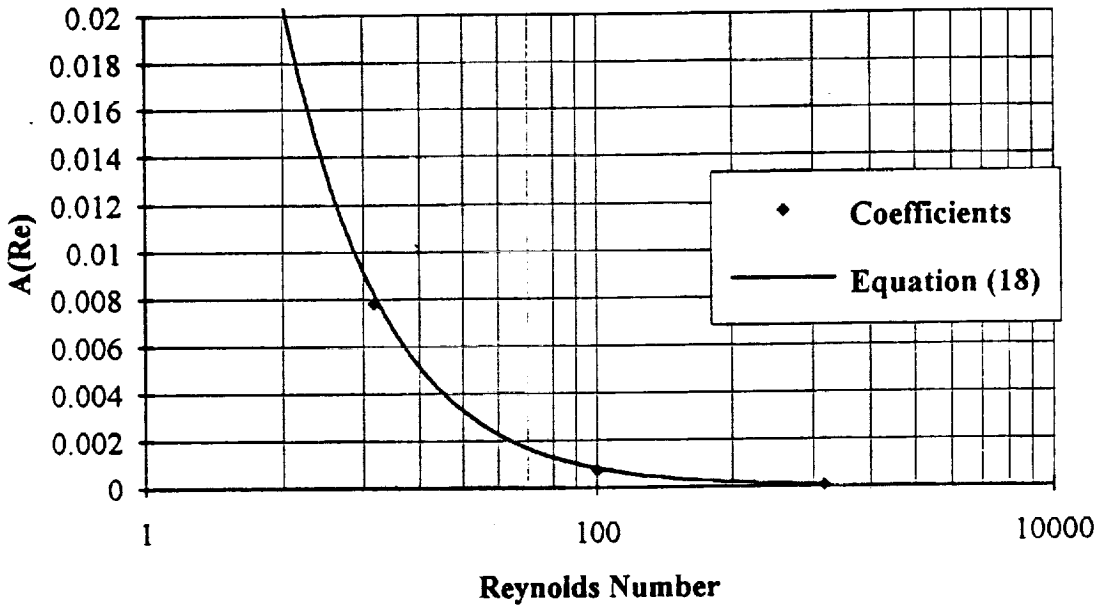

Figure 7
Expansion/Contraction Correction

A similar analysis was performed to determine the coefficient for Strouhal Number dependence. The resulting least squares fit is given by

$$C(S_t) = 1.0 + 0.032 S_t^{0.677} \tag{19}$$

and is shown in Figure 8. Notice that the coefficient approaches 1 for low Strouhal Number (steady flow), as expected, and increases with increasing Strouhal Number.

Other coefficients can be developed for Expansion Ratio and Radius to Diameter Ratio. A comparison of the model predictions to FIDAP simulations is shown in Figures 9 and 10. The good agreement indicates that the assumed separation given in equation (17) produces reasonable results.

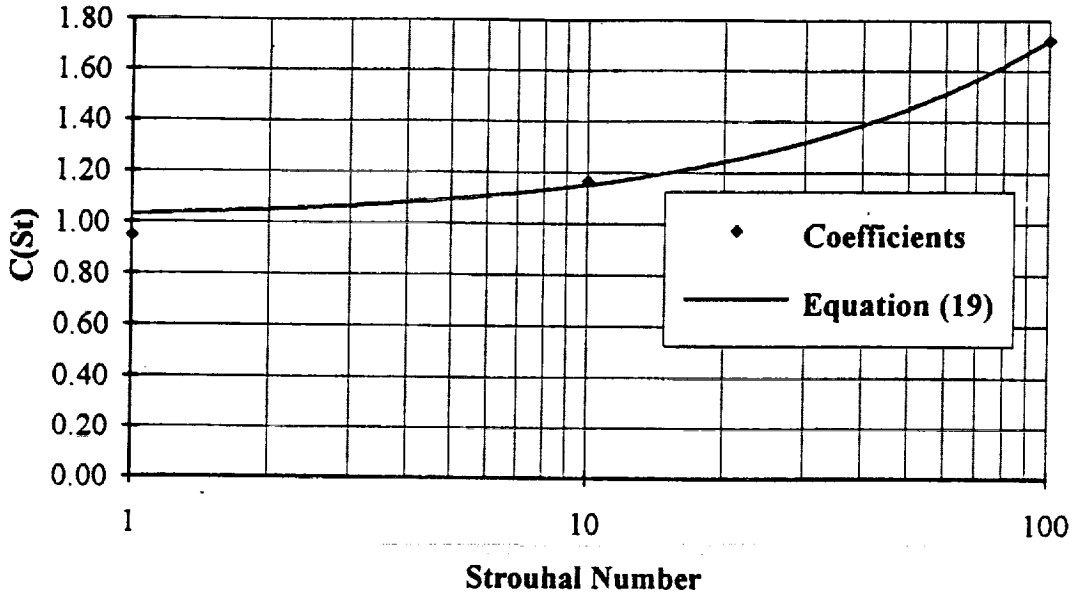

Figure 8
Expansion/Contraction Coefficient vs. Strouhal Number

Track Coefficients

As previously discussed, the theoretical model for the track was derived for periodic fully developed pipe flow. In the developing region the viscous stresses are higher because the velocity profiles are more uniform. The theoretical model will therefore underpredict the pressure drop in this region. For long pipes this error will be negligible; however, the error will increase as the length of pipe decreases. The coefficient for this correction is shown in Figure 11 and given by

$$C(l/d) = 1.0e^{\left[\frac{0.078}{(l/d)^{0.604}}\right]} \tag{20}$$

For noncircular cross sections the concept of an equivalent diameter is used. Pressure drop in the inertia track correlates well with Valenci number. At high Valenci numbers the pressure drop is mostly inertial, and thus a function of cross sectional area and independent of cross sectional shape. At lower Valenci numbers the cross sectional shape can significantly influence pressure drop. The equivalent diameter ratio (defined as the diameter of a circle that gives the same pressure drop divided by the diameter of a circle of the same area as the rectangle) for various aspect ratios of a rectangular cross section are shown in Figure 12. As expected, the coefficients asymptotically approach 1 at high Valenci number. The Figure also shows that the pressure drop in a square cross section is almost equivalent to that in a circular

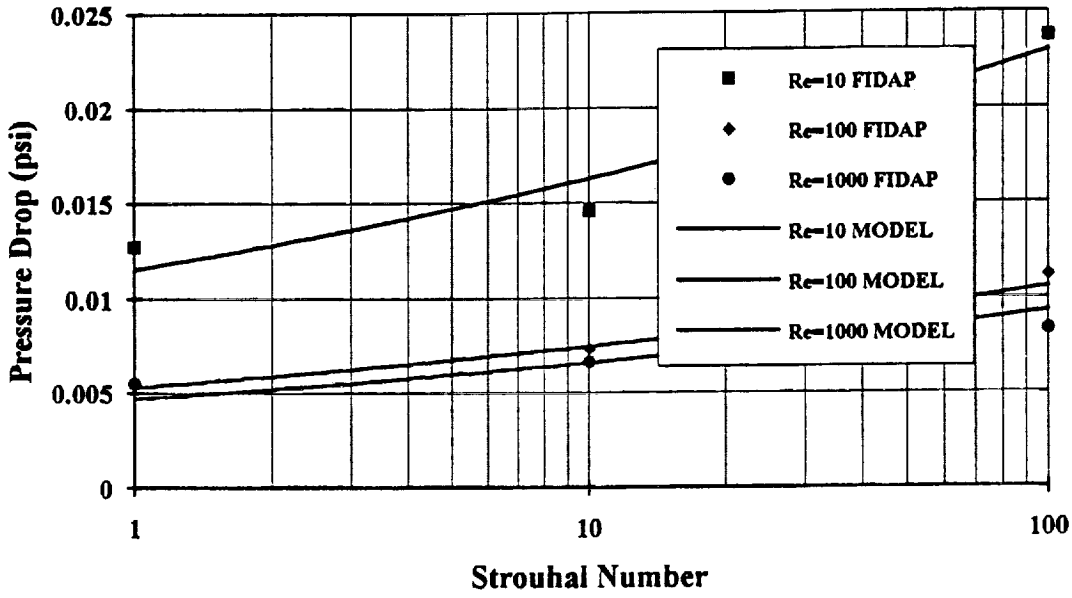

Figure 9
Expansion/Contraction Pressure Drop vs. Strouhal Number Using Corrected Model

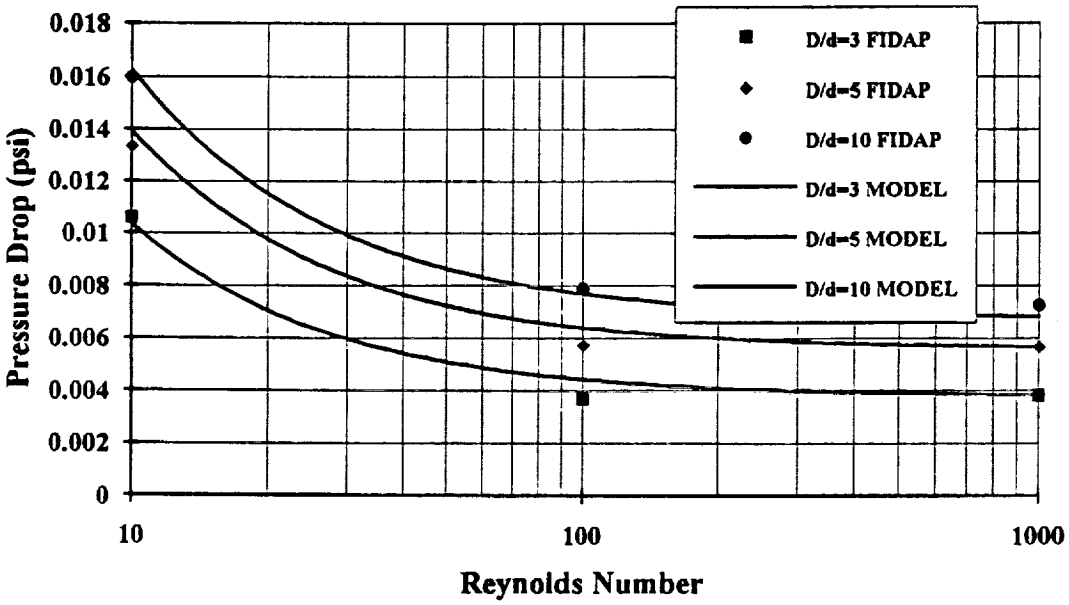

Figure 10
Expansion/Contraction Pressure Drop vs. Reynolds Number Using Corrected Model

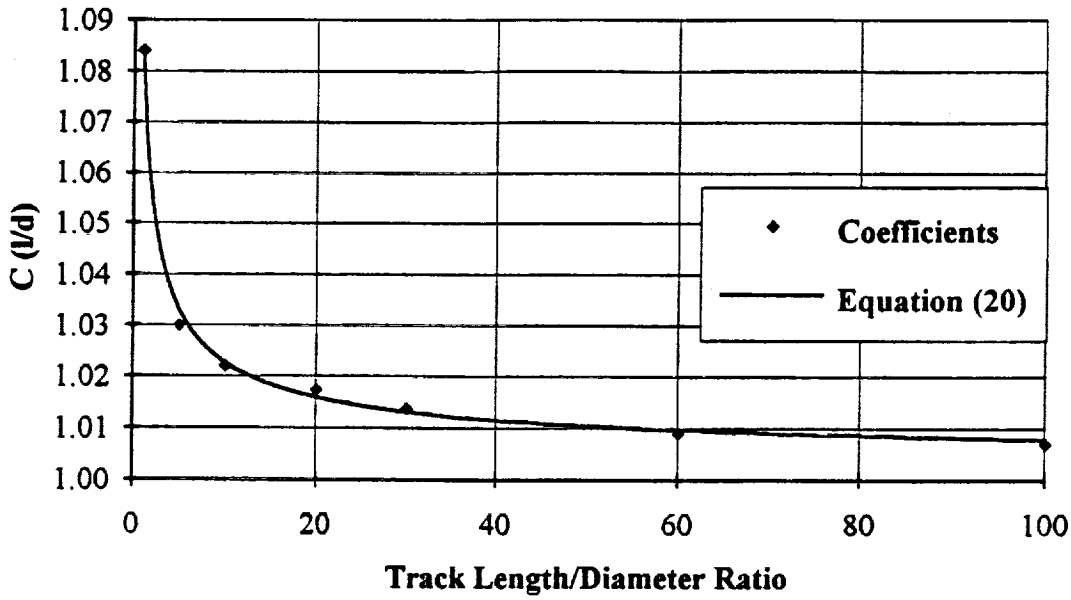

Figure 11
Track Coefficient vs. l/d

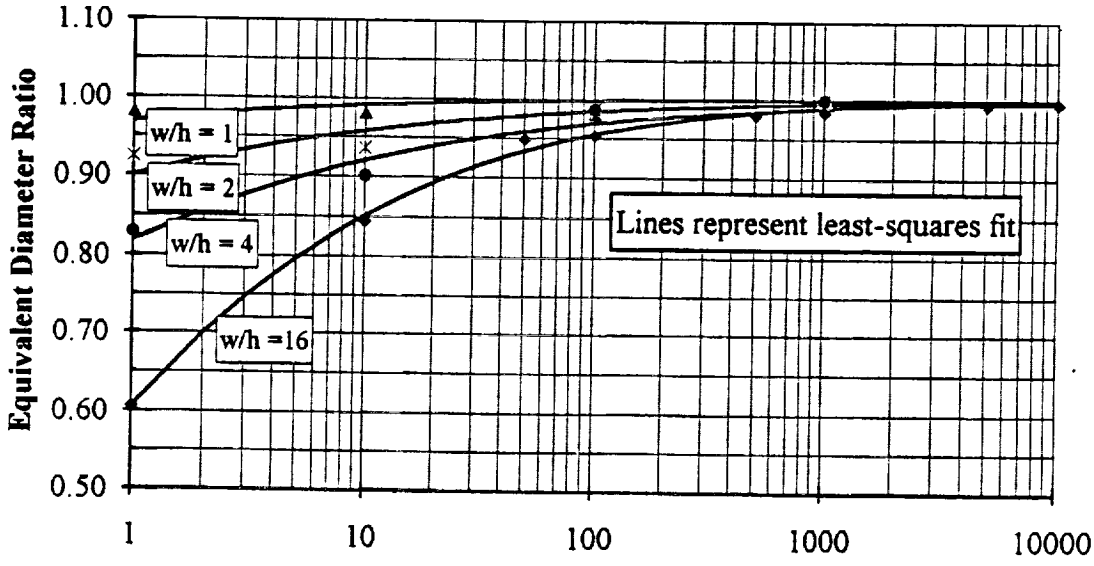

Figure 12
Equivalent Diameter Ratio for Rectangular Cross-Section

cross section of equal area, and increases as the aspect ratio increases.

Coefficients similar to the ones described here can be developed for more complicated geometries. These coefficients will expand the applicability of the model to realistic mount geometries. Work is currently in progress to develop these coefficients.

CONCLUSIONS

A series of component models have been developed for predicting the pressure drop in fluid tuned mounts. Empirical coefficients that will expand the applicability of the models have been developed, and predictions from the adjusted models agree well with computational simulation. As additional coefficients are developed the model will become more useful in the design of realistic mounts.

A major obstacle to completing this model is the problem of determining critical Reynolds number. Further research, including experimental verification, is in progress.

ACKNOWLEDGMENTS

This work was supported by the LORD Corporation and the Ben Franklin Partnership of Pennsylvania.

REFERENCES

1. Flower, W., "Understanding Hydraulic Mounts for Improved Vehicle Noise, Vibration and Ride Qualities", SAE Paper #850975, (1985)
2. Gerhart, P.M. and Gross, R.J., "Fundamentals of Fluid Mechanics", Addison Wesley, Reading, MA. (1985)
3. Wormersley, J.R., "Method for the Calculation of Velocity, Rate of Flow, and Viscous Drag in Arteries When the Pressure Gradient is Known", J. Physiol., **127**, 553-563, (1955)
4. Abramowitz, M. and Stegun, I.A. "Handbook of Mathematical Functions", Dover Publications, N.Y. (1972)
5. Khalilollahi, A., Lasher, W.C. and Weckerly, D.E., "Mathematical Modelling of Fluid Filled Isolator Mounts", submitted for publication in Int. J. of Modelling and Simulation
6. FIDAP Manuals, Fluid Dynamics International, Evanston, IL. (1990)
7. Ahn, K.H. and Ibrahim, M.B., "Laminar/Turbulent Oscillating Flow in Circular Pipes", Int. J. of Heat and Fluid Flow, 13, #4, 340-346, (1992)
8. Lasher, W.C. and Taulbee, D.B., "On the Computation of Turbulent Backstep Flow", Int. J. of Heat and Fluid Flow, 13, #1, 30-40 (1992)
9. FLUENT Manuals, FLUENT, Inc., Lebanon, NH. (1992)